Link Quality Fluctuation in Wireless Networks Deployed on the Surface of Different Water Bodies

Waltenegus Dargie (iD), *Senior Member, IEEE*, Paulo Padrao (iD), Leonardo Bobadilla (iD), and Christian Poellabauer (iD), *Senior Member, IEEE*

Abstract—Low-power IoT sensing nodes can be deployed on the surface of different water bodies for various purposes, including water quality monitoring and pollution detection. Two of the most formidable challenges towards such goals are (1) making the nodes resilient against rough water and extreme weather conditions, and (2) enabling the nodes to establish reliable wireless links. In this paper we share our experience in deploying low-power and resilient IoT nodes on the surface of different water bodies – on a small lake, North Biscayne Bay, Crandon Beach, and South Beach, in Miami, Florida. Furthermore, the paper closely examines how link quality was affected by pre-deployment configurations as well as the characteristics and the motion of the waters. Based on the analyses of a vast amount of statistics, the paper establishes a theoretical (mathematical) and generalized model to characterize and predict link quality fluctuations. We shall show that the realization of the model using the Kalman Filter enables link quality prediction with accuracy exceeding 90%.

Index Terms—Water quality monitoring, wireless sensor networks, Internet of Things, link quality fluctuation, RSSI. surface water deployment

I. INTRODUCTION

Water is a precious and scarce resource. When the quality of a body of water deteriorates, the consequences are often far-reaching and long-lasting [1]. In some continents, water is a frequent cause of tension and conflict, both between and within nations [2]. The factors affecting water quality can be natural or man-made. Some of the most significant natural factors are climate change, a significant rise in water temperature worldwide, and heavy rainfall causing sediment and nutrient fluxes and pollution to overflow water bodies. Some of the most significant man-made factors include improper solid and liquid management, urbanization, fast population growth, agricultural intensification, and reliance on harmful fertilizers which may eventually end up in water bodies [3].

Scalable and sustainable water quality monitoring is crucial to ensure the well-being of water bodies. One of the most

formidable challenges associated with deploying cost-effective water quality monitoring systems is that some of the sensing nodes have to be deployed on the surfaces of rough and restless water bodies, which severely affect the wireless links the nodes establish. As the first contribution of this paper, we offer rich experimental insights into this challenge. To the best of our knowledge, ours is the most comprehensive study involving the deployment of low-power wireless sensing networks on the surface of different water bodies. The paper addresses the impact of experimental setups on the performance and stability of the wireless links. While the rough motion of the surfaces of water bodies is the main cause of link quality deterioration, device imperfections, impedance mismatch, and other hardware/system configuration aspects further exacerbate link quality fluctuation. The second contribution of the paper is establishing a theoretical (mathematical) and generalized model to express and predict link quality fluctuations in deployments involving rough and restless water surfaces.

The rest of this paper is organised as follows: In Section II we discuss water quality monitoring in different contexts. In Section III, we discuss our experiment settings and network configurations. In Section IV, we present some interesting pre-deployment observations. In Section V we present a detailed account of link quality fluctuation as a result of deploying wireless sensor networks on the surface of a lake, Atlantic Ocean, and North Biscayne Bay. In Section VI we discussed papers which undertook similar studies as ours. Finally, in Section VII we outline future work and give concluding remarks.

II. WATER QUALITY MONITORING

Water quality monitoring takes place in different ways. The first approach relies on laboratory tests, after water samples are collected manually. This approach, though widely employed, requires skilled personnel [4] and it is time-consuming, tedious, inconsistent, and unreliable. The second approach is automated and consists of monitoring and control stations/substations permanently deployed at various locations [5]. A substation collects representative samples from a particular body of water and a station aggregates the data from multiple substations. A control station controls and manages multiple monitoring stations [6]. This approach is reliable but not widespread. Typically, it is deployed in a limited number of critical water bodies supplying drinking water. The third approach relies on remote sensing [7]–[9]. Here, the spectrum of electromagnetic waves radiating, reflected, and/or scattered

from water bodies is analyzed to extract several features. While capable of monitoring extensive water bodies, it is, however, expensive and highly affected by weather and other environmental factors [10].

The fourth approach is in situ monitoring [11] in which physical sensors are deployed to directly sample and evaluate water quality. It may be carried out in different ways (by deploying boats, Unmanned Surface Vehicles, buoys, etc.), but involves expensive devices and setup. For example, Florida International University (FIU) has deployed five research buoys (not related to this work) in strategic locations (Coral Gables Canal, Little River, Miami River, North Biscayne Bay, and Biscayne Canal) to measure eight water parameters (pH, temperature, conductivity, dissolved oxygen, turbidity, chlorophyll, fluorescent dissolved organic matter, and directional flows peed)[1] which are sampled every 15 minutes and transmitted to a cloud server via satellite links. Since the distance between the buoys is several kilometers, the Institute of Environment carries out a boat tour twice a month (and whenever interesting events are detected) to take samples from several locations at a much higher spatio-temporal resolution. The mobile as well as the stationary sensing and data logging devices are price-intensive, each of which costs more than $20,000.

A more affordable and scalable water quality monitoring is necessary to achieve scalable and ubiquitous sensing. Towards this end, two formidable challenges have to be overcome. The first concerns the sensing task. Both affordable and highly reliable water quality sensors are essential. The second challenge concerns wireless communications. Most of the water quality monitoring devices are either deployed or have components which are deployed on the surface of water. These devices should be able to endure the rough movement of water and function in extreme weather conditions. In this paper we shall share our expedience with deploying low-power wireless sensor networks on the surface of different water bodies.

III. EXPERIMENTAL SETTING

We identified four different locations in Miami, Florida, to investigate the predominant factors that affect the link quality of low-power networks deployed on the surface of a water body. The first location was one of the lakes on the Florida International University (FIU) main campus. Situated in front of the School of Computing and Information Sciences, the lake is calm, but three fountains in the middle of the lake cause constant ripples in all directions. The second location was North Biscayne Bay, which is a lagoon with characteristics of an estuary, located near Miami. Here the water is salty. When there are no boats around, the water is relatively calm, otherwise, it makes considerable and random ripples. Of late, the quality of the bay has been deteriorating on account of several external causes (a rise in temperature, low tide, heavy rainfall, and sanitary sewer overflow, among others), which resulted in a considerable algae bloom and the death of a large quantity of fish and other species [12], [13]. Our third and fourth locations were South Beach, Miami, and Crandon
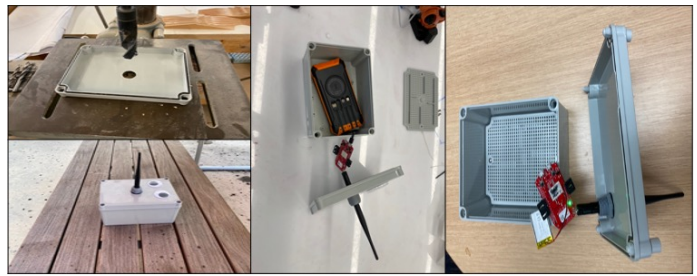

Fig. 1: A wireless sensor node placed in a waterproof box and deployed on the surface of water.

Item	Capacity	Cost
Waterproof box	ca. 335 cm^3	$10
Herdio Waterproof Marine Antenna	ca. 15 cm high above the water surface	$16
IMu	9 DOF	$10
Zolertia platform	CC2538 SoC (2.4 GHz), CC1200, sub-GHz	$190
Big power bank	30000 mAh, integrates solar panel	$50
Small power bank	6000 mAh	$10

TABLE I: Description and cost of the components we used to build our sensing buoy.

Beach, Miami, respectively. In both locations, the water was salty, the waves were large, and the direction of the wind changed appreciably.

The sensor networks we deployed were of two types. The first type consisted of nodes placed in open floating boxes, while the second consisted of nodes sealed in waterproof boxes. This differentiation was important in order to quantify the cost we incurred (in terms of the performance degradation of the wireless links) when we sealed the sensor nodes in waterproof boxes (we sometime refer to these nodes as buoys). Fig. 1 displays a sensor prototype. Tab. I summarizes the description and cost of the components we put together to setup the sensing buoys. The nodes can be deployed with small or big power banks. One of the big power banks we used, besides having 30000 mAh capacity, added weight to the buoy to make it stable. Where the water body is relatively calm, more affordable and lighter power banks can be used (as shown in Fig. 1 (right)).

Fig. 2 shows the wireless sensor networks we deployed with

Fig. 2: A wireless sensor network consisting of nodes placed inside open floating boxes and deployed on the surface of different water bodies.

---

[1]https://crestcache.fiu.edu/research/research-buoys/

Fig. 3: A wireless sensor network (with nodes sealed in waterproof boxes) deployed on the surface of different water bodies.

open floating boxes on a lake on the FIU main campus and in North Biscayne Bay. In addition to the essential differences in terms of the waters characteristics (sweet versus salty; water motion), the two settings differ from each other in terms of the cross-technology interference (CTI) the wireless sensor networks experienced. FIU's main campus has an extensive WiFi coverage, which affected the performance of our networks considerably. Similarly, Fig. 3 displays the deployment of buoys in three different settings (lake, South Beach, and Crandon Beach).

A. Radio Technologies

Our sensor nodes integrate two types of radios: CC1200 and CC2538. The CC1200, a sub-GHz IEEE 802.15.4 radio, can operate at different sub-Gigahertz frequency bands (868, 915, 920, 950 MHz) and is capable of data buffering, burst transmissions, clear channel assessment, and Wake-On-Radio[2]. It can transmit at a maximum power of 16 dBm and has a sensitivity of -123 dBm. Although theoretically it can achieve a maximum transmission rate of 1.25 Mbps and a maximum transmission range of 4 km, our experience suggests that the practically achievable values are much less than the nominal values, depending on both environmental factors and network configuration (network size, network topology, packet size, etc.). With a network size of 6, a linear topology, and a packet length of 128 bytes, the stable transmission rate we could achieve was less than 40 kbps and a transmission range less than 1 km. Similarly, the CC2538 system-on-chip integrates a 2.4 GHz IEEE 802.15.4 compliant RF transceiver having a sensitivity of –97 dBm and an adjustable output power (reaching up to 7 dBm). The radio can transmit at 250 kbps nominal rate and, compared to the CC1200 radio, is much more stable. However, for most practical purposes, the achievable transmission range is less than 100 m in free space.

B. Network Configuration

In our networks, the nodes self-organized using the RPL Lite protocol implementation in the Contiki operating system [14]; medium access was achieved using CSMA/CA. All

nodes transmitted packets towards the base station, which was also the root node in the RPL hierarchy. Each time a node received a packet from its neighbors, it extracted the RSSI and LQI with which it received the packet, and added a corresponding timestamp to this piece of information. Initially, the nodes sent to their neighbors a simple "HELLO" message, but afterward embedded in the payload of the packet they transmitted the link quality metrics of the packet they received from their immediate neighbors most recently, along with two additional metrics: the number of packets they had transmitted and the number of packets they had lost up to that point. For all experiments, the packet length was 128 bytes. When using the CC1200 chip, nodes transmitted at 2 Hz rate; when using CC2538, they transmitted at 10 Hz rate.

IV. INITIAL EXPERIMENTS

Initially, we undertook several experiments to obtain reference values and to quantify the effects of various factors on the performances of the networks. As previously mentioned, we had two types of power banks with different heat dissipation profiles; open and sealed boxes; land versus surface water deployments; and sweet versus salt water deployments. Moreover, the water bodies exhibited both translational and back-and-forth (local) motions whose magnitude and movement patterns differed.

A. Effects of Waterproof Boxes

The most important factor for our choice of waterproof boxes was their price. Since all deployments were going to take place in Miami, Florida, the boxes had to protect the sensor nodes from excessive external as well as internal heat (dissipation) as well as from harsh weather conditions (heavy rainfall and high humidity). We were, however, equally concerned about the boxes, that they did not significantly affect (attenuate) the electromagnetic signal propagation and reception. Although this concern was partially addressed by the use of the waterproof marine antennas, the effect of the boxes still had to be examined. Consequently, we carried out multiple point-to-point communications, both on land and on the surface of water. Each experiment was repeated at least 5 times and with different pairs of persons. For the experiments on land, we placed one of the sensor nodes on the ground and the other was carried (at a height of ca. 1.5 m) by a person walking at a pace of ca. 1.4 m/s away from the ground node, continuously maintaining a line-of-sight. The person moved until the link was permanently broken (i.e., the nodes were unable to reestablish a link afterwards). We measured distance and compared the link quality fluctuations of the different configurations (with and without the waterproof boxes and with big versus small power bank).

Intuitively, one would expect that the link quality would be better when the boxes were not sealed. But this was not what we experienced. The link quality was consistently better, and the transmission range was consistently longer, when the nodes were sealed inside the waterproof boxes. This was true regardless of the radios used. In order to exclude the hot

---

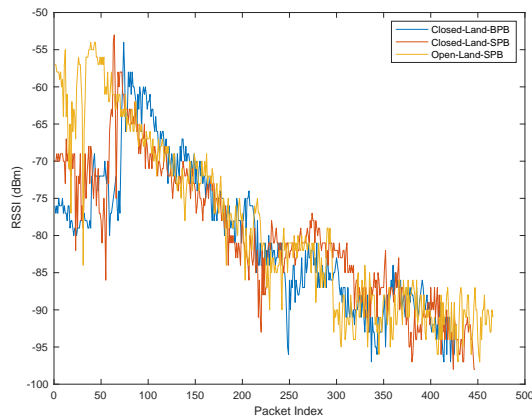[2]https://www.ti.com/product/de-de/CC1200 Last visit. August 31, 2024, 11:400 AM, CET.

Fig. 4
Link quality variation on land for different configurations (CC2538, 2.4 GHz radio). BPB in the legend refers to Big Power Bank and SPB refers to Small Power Bank.[3]
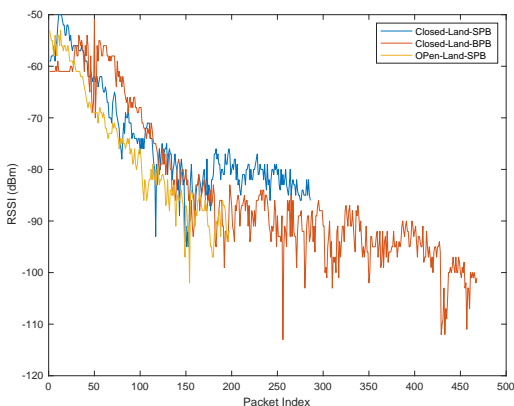

Fig. 5: Link quality variation on land for different configurations (CC1200, 868 MHz radio). BPB in the legend refers to Big Power Bank and SPB refers to Small Power Bank.

weather as the main cause of poor performance in the unprotected nodes (in the open boxes), we repeated the experiments both early in the morning and late in the afternoon, when the temperature was relatively mild, but the results were, by and large, the same. Hence, the most reasonable explanation for the slightly improved performance in the waterproof boxes is that the sensor platforms were protected from electromagnetic interference.

Fig. 4 shows the link quality fluctuation (reflected by the variation in the RSSI values of received packets) for three different configurations corresponding to the experiments conducted on land. The long-term RSSI variations clearly reflect the relationship between the received power and the distance. Apparently, the short-term variations were due, partly, to the movement of the persons (the arms) holding the nodes. For the three configurations (open with the small power bank; sealed with the small power bank; sealed with the big power bank, re-

---

³The plots in Figs. 4 - 6, 13 are produced as follows: Packets were given sequence numbers and transmitted in succession. Upon receiving these packets, their RSSI values were measured and associated with their sequence number (index). Hence, the plots describe RSSI vs. Packet Index.
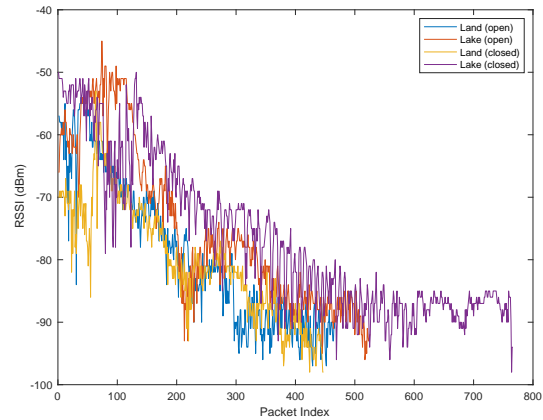

Fig. 6: Link quality variation on land vs. lake for open-box vs. closed-box (i.e., sealed-box) configurations (CC2538, 2.4 GHz radio). The small power bank was used for these experiments.

spectively) the average transmission ranges we observed were the following: 48.8 m, 57.8 m, 75.2 m. The corresponding standard deviations were: 9.60, 10.96, 12.11 m. Note that the transmission range may not be apparent from the plot due to the presence of some degree of randomness (both in pace and stride) in the walking pattern of the persons. Fig. 5 shows the link quality fluctuation in the three different configurations when the CC1200 radio was used for the land experiments.

B. Big versus Small Power Banks

For this comparison, we consider the waterproof platforms. The small power bank was a 3.7 V lithium-polymer 503040, capable of delivering 600 mAh. The bigger power bank was a PN-W22 GOODaaa, capable of delivering 36000 mAh. Both were fully charged before each experiment, and the radios were transmitting with their maximum power. For both settings, the experiments lasted much shorter than the times the power banks took to exhaust their energy. In other words, the difference in the energy reserve between the two power banks should have played no significant role on the quality of the links the nodes established. This, however, was not what we experienced. In all the experiments we conducted, the quality of the wireless links was noticeably better, and the communication range was consistently longer, when the big power bank was employed, as can be seen in Figs. 4 and 5. This is, in part, due to device imperfection, a problem which is widely discussed in the literature [15]–[17]. This imperfection is often manifested in the form of an impedance mismatch between the output impedance of the power bank and the input impedance of the sensor platform (maximum power transfer occurs when the input impedance equals the output impedance) [18]. The cheaper the power bank, the more likely the mismatch.

C. Water Characteristics

We repeated the experiments open vs. sealed boxes on the lake at FIU. In these experiments, we attached the open and sealed boxes to a long rope. One end of this rope was on the
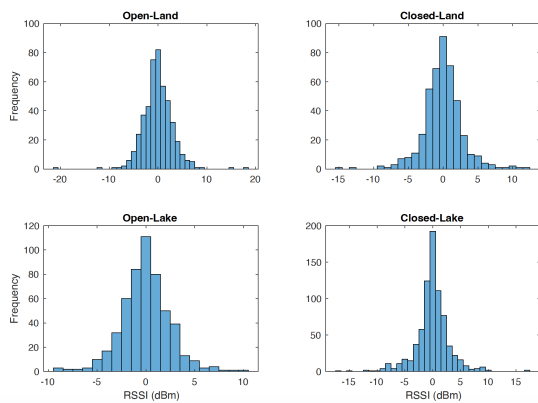
Fig. 7: Histogram of the change in Link quality ($RSSI_t - RSSI_{t-1}$) on land vs. lake for open-box vs. closed-box (i.e., sealed-box) configurations (CC2538, 2.4 GHz radio). The small power bank was used for these experiments.
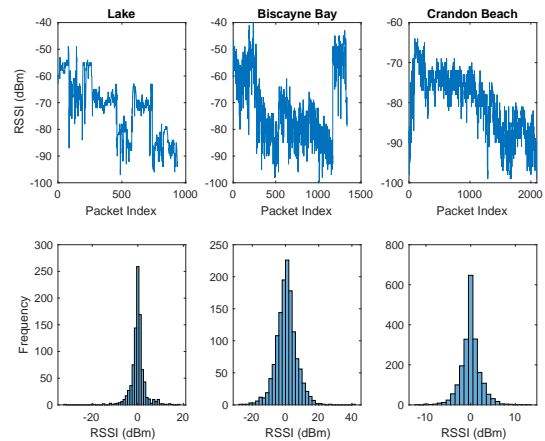

Fig. 8: The change in RSSI for three different wireless links. The plots on the top show the raw data, whereas the plots at the bottom summarize the change ($RSSI_t - RSSI_{t-1}$) with histograms.

other side of the lake. At the beginning of the experiments, the transmitter and the receiver were near to each other. Then, the sealed box containing the transmitter was slowly (ca. 0.25 m/s) pulled away by a person on the other side of the lake whilst the two nodes communicated. The pulling stopped when the links between the nodes were permanently broken. On average, deployments on the lake had a superior performance compared to those on land and the best performance was achieved when the sealed boxes were used, as shown in Fig. 6 (the small power bank was used in all the experiments). One way to compare the difference in link quality between the different configurations would be to differentiate the raw RSSI values with respect to time and evaluate the statistics thereof. This way, we can confine our evaluation to short-term variations (the degree to which neighbor values differ from one another). Fig. 7 compares the histograms of the short-term link quality variation for the four different configurations. The figure suggests that the variation was the smallest for the deployment of the buoy (the closed configuration) on the lake.

V. IMPACT OF WATER MOTION

The motion of water affects the nodes in many respects. Some of the most important effects are link quality fluctuation and a change in the physical topology of the network, which, in turn, affects how nodes self-organize and cooperate. In the pre-deployment phase, we established that there is a correlation between the change in the RSSI of successfully transmitted packets and the movement of the nodes. However, the complexity of the motion the nodes experience and its impact on the signal's propagation and multi-path scattering greatly depend on the characteristics of the water. Fig. 8 displays the change in the RSSI of three different wireless links for deployments which took place in three different locations (lake, Biscayne Bay, and Crandon Beach). In all the cases, the waterproof buoys were employed. In order to evaluate the relative change the buoys experienced as a consequence of the motion of water, we differentiated the raw values and plotted their statistics (histograms). The motion of the buoys on the lake and on the bay was restricted by

the ropes to which the they were tied. In Crandon Beach, on the other hand, the buoys were free to drift. At the time of the experiments, all the waters were experiencing motion, the waters of the bay and Crandon Beach more significantly. The main differences between the motions of the waters of the bay and Crandon Beach was that the waves of the latter were higher in magnitude and shorter in wavelength[4]. These characteristics are to some extent reflected in the histograms.

The integration of 3D accelerometers and 3D gyroscopes into the sensing platforms enables to examine the existence of a correlation between the motion of water and the change in the link quality. If there is a perceivable cause-and-effect dependency between the two, then it is plausible to assume that the link quality is predictable. A predictable link quality is an essential prerequisite to carry out adaptations at different abstraction layers: At the physical layer, it enables dynamic transmission power adaptation; at the MAC layer, it enables efficient packet transmission scheduling; and at the network layer, it enables to discover new routes and adapt to changes to the network's topology. Fundamental to all is that the dependency (1) has a theoretical (mathematical) bases and (2) can be generalized.

A. Simulated Motion

As we did in the pre-deployment phase, we carried out two sets of experiments on land to establish ground truth. The first set was intended to establish the change in the RSSI of successfully transmitted packets in the absence of any movement. We model this change as a measurement error. We surrounded the lake on FIU's main campus with 10 sensor nodes. The distance between the nodes was about 50 m. RPL was used as the routing protocol. After the experiments, we differentiated the RSSI values to determine the change. Assuming that all external factors (such as weather) remained

---

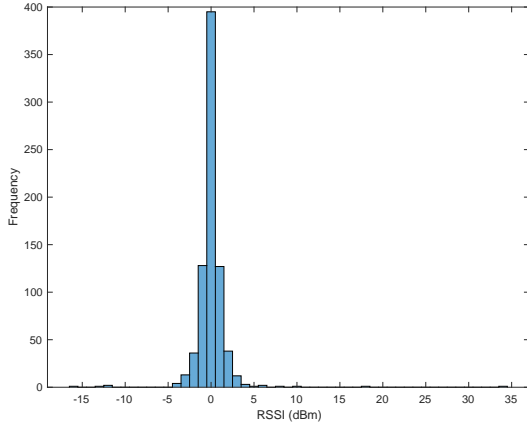[4]A video of the deployment at Crandon Beach can be found at: https://youtu.be/u9JWtoZWSNw

Fig. 9: Histogram of the change in the RSSI values in the absence of movement. This change is regarded as a measurement error.
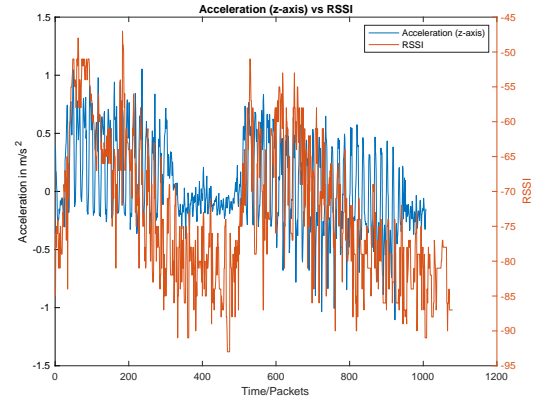

Fig. 10: Variation in RSSI values of received packets and a corresponding variation in linear acceleration (along the z-axis) of a swinging buoy during a simulated movement.

constant, this change reflects the uncertainty associated with the measurement only. To determine the change in the RSSI due to the movement of water, this error has to be first subtracted. Fig. 9 displays the histogram of the measurement error we established by aggregating the RSSI values of all single-hop links. As can be seen, this change can be modelled as a normally distributed random variable, which can be expressed in terms of its mean and variance alone.

In the second set of experiments, the aim was to:

1) distinguish between the effects of water motion and multi-path scattering; and,
2) establish correlation between the change in the RSSI and the change in the linear acceleration and angular velocity the nodes experience.

In these experiments, one of the nodes was stationary and the other (the transmitter) was carried by a person moving at a normal pace away from the stationary node, frontal plane orthogonal to the direction of movement. While moving away, the person swung the node sideways, imitating the movement of a node tossed back and forth by the passing of water waves. In order to ascertain that the effect of acceleration is visible, the person stopped at some distance (13 m for the CC2538) for a while; moved some distance (7 m for CC2538) back without swinging the node; and proceeded swinging the nodes while moving forward, until the connection was broken. The experiment was repeated 5 times for each radio. Fig. 10 displays the change in the RSSI and the corresponding change in the linear acceleration along the z-axis for one of the experiments, clearly suggesting that the two are correlated.

B. Theoretical Model

Following the experiments with the simulated movement, we carried out several deployments at South Beach and Crandon Beach to investigate the change in link quality as a result of the buoys' interaction with water in motion. Fig. 11 shows the histograms of the changes in the RSSI values of successfully transmitted packets for the CC2538 and CC1200 radios for one of the experiments carried out at Crandon
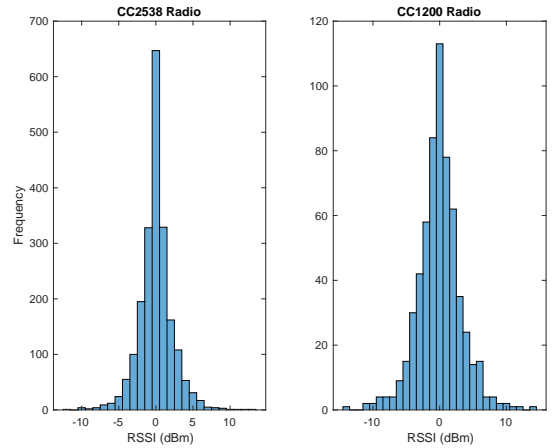

Fig. 11: Histograms of the change in RSSI ($RSSI_t - RSSI_{t-1}$) of received packets for the CC2538 (left) and the CC1200 (right) radios for one of the deployments carried out at Crandon Beach.

Beach. The plots suggest that the process error in both cases can be regarded as a normally distributed random variable. If we consider this observation along with the observation we made with respect to the measurement error (see Fig. 9), it seems reasonable to employ the Kalman Filter to predict the change in the RSSI.

Thus, using the Kalman formulation, the best estimation of the change in the RSSI at the time instant t can be expressed as:

$$\hat{r}(t) = r_p(t) + K(t)\left[r_m(t) + r_p(t)\right] \tag{1}$$

where $r_p(t)$ refers to the error due to the prediction made for time t based on whatever knowledge we had at time $t - 1$; $r_m(t)$ is the measurement error at time t and,

$$K(t) = \frac{P(t)}{P(t) + R} \tag{2}$$

where $P(t)$ is the variance of the prediction error and R is the variance of the measurement error. R is supposed to be time

$$P(1) = Q \qquad P(2) = C(1) + Q$$
$$r_p(1) = x_m(0) \qquad r_p(2) = \hat{r}(1)$$

$$t = 0 \qquad t = 1 \qquad t = 2$$
$$r_m(0) \qquad r_m(1) \qquad r_m(2) \qquad \ldots$$

$$C(1) = P(1) + Q$$
$$K(1) = \frac{P(1)}{P(1) + R}$$
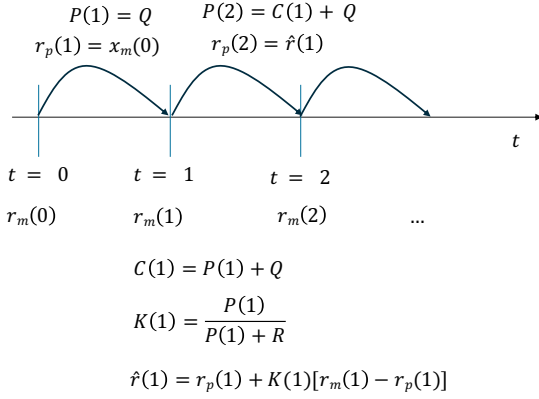$$\hat{r}(1) = r_p(1) + K(1)[r_m(1) - r_p(1)]$$

Fig. 12: Algorithm for the Kalman Filter.

invariant. The prediction error consists of two components, since:

1) the prediction is made based on uncertain past knowledge, this is described by $C(t-1)$;
2) the system's future state is inherently uncertain (contains randomness), this is described by the variance of the process error, Q, which is supposed to be time invariant.

Hence,

$$P(t) = C(t-1) + Q \tag{3}$$

One of the strengths of the Kalman Filter is its ability to connect the past, the present, and the future by describing the overall accumulated error in our estimation up to time t as follows:

$$C(t) = [1 + K(t)]^2 P(t) + K(t)^2 R \tag{4}$$

For a more elaborate discussion on the Kalman Formulation, we refer the reader to [19]. Fig. 12 summarizes our Kalman Algorithm. In the beginning, we have only $r_m(0)$, R, and Q. Therefore, our best estimate of $\hat{r}(0) = r_m(0)$. Likewise, since no estimation is accumulated so far, our prediction error consists only of Q. Thus, $P(1) = Q$. With this, we are ready to compute the following for $P(2)$:

$$K(1) = \frac{P(1)}{P(1) + R} \tag{5}$$
$$C(1) = [1 + K^2(1)]P(1) + K^2(1)R$$
$$P(2) = C(1) + Q$$

In Fig. 13, three plots are compared with one another for the two radios. The plots in red refer to actual measurements we obtained; the plots in green refer to actual measurements minus measurement errors, assuming that the error in both cases was normally distributed. The plots in blue refer to the predictions we made using the Kalman Filter.

The application of Kalman Filter to predict link quality fluctuation in deployments involving different water bodies and radio chips confirms that theoretical and generalized models can be established to express and predict link quality fluctuation and to support adaptation. The prediction root mean square error ($\sqrt{E\{[r(t) - \hat{r}(t)]^2\}}$), taking the predictions for

all the times and the deployments into consideration, is ca. 10%, with standard deviation of 1.3%.

VI. RELATED WORK

Low-power IoT systems are being increasingly deployed in rough outdoor environments [20]. The work presented in [21] explores the effects of water surfaces on radio communications in the 300 MHz - 3 GHz range. The paper discusses real-world measurements collected on the Yangtze River (freshwater) and on a beach in the East China Sea (salt water) to demonstrate how different water surfaces backscatter radio signals due to material and hydrodynamic variances. While our work focuses on sensor devices placed directly on the water surface, the work in [21] focuses on radio devices that were placed between 17 and 50 meters above the water surface. A similar study was performed in [22], which also observes that recurrent natural phenomena (tides or waves) cause shifts in the water level, changing the interference patterns and causing varying impairments to propagation over water surfaces. Experiments were performed between a device onshore and another one on the water surface, using the 2.4 and 5 GHz bands. The primary outcome of the research is a method to determine optimal link distance and height combinations, which may not be applicable to sensor networks with devices that always float directly above the water surface. The focus of the work presented in [23] is to develop a path-loss model for wireless communications in open-sea environments that considers various effects, such as reflection, shadowing, divergence, and diffraction caused by the sea surface. The work includes measurements performed in cold and calm waters near Norway to validate the developed model for long-distance communications (up to 45 km). A similar effort to develop a path loss model was presented in [24]; however, communications over short distances (i.e., up to 60 m) and analyzing the impact of water temperature on radio transmission quality were the focus of this study.

Unlike previous studies that evaluate RF propagation over water but did not distinguish maritime-specific factors from factors affecting terrestrial RF systems, the work presented in [25] carried out RSSI data collection over land and seawater at 2.4 and 5 GHz bands using different antenna heights. The findings reveal that transitioning from land to seawater with certain combinations of frequency bands and antenna height leads to a path loss of 2 to 3 dBm. These insights can be valuable for optimizing the performance of wireless communication links, particularly, in scenarios with heterogeneous teams of mobile sensing systems [26], [27]. Overlooking or oversimplifying the complex behavior of ocean waves significantly impacts the stability of wireless links between sensors [28]. In the work presented in [29], the authors determine the likelihood of line-of-sight (LoS) link blockages between transmitter and receiver pairs, considering the effects of wave movements, and perform an examination of how environmental variables, such as wind speed, affect this probability. These outcomes provide feasible avenues for reducing variations in low-power wireless communications through enhanced wave modeling and the incorporation of environmental factors.
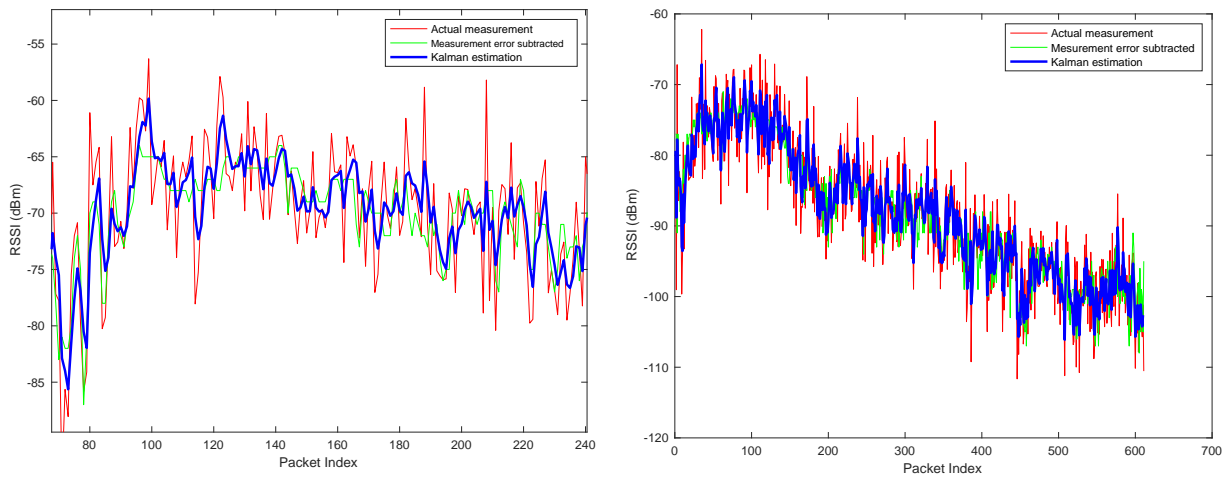
Fig. 13: Prediction of link quality fluctuation using the Kalman Filter. Left: Snapshot of the predicted values of the simulated motion. Radio: CC2538. Right: For a measurement taken at Crandon Beach. Radio: CC1200.

A deployment closely related to our current work is presented in [30], where 10 floating buoys housing 10 sensor nodes were deployed in the shallow waters of Moreton Bay, Queensland Australia. The wireless sensor platforms integrated illuminance and temperature sensors and IEEE 802.15.4 compliant 2.4 GHz radios. The authors reported that, despite strong tidal current conditions, communication between the buoys was successful, they, nevertheless, did not provide a detailed account of the extent to which the wireless links were reliable.

VII. Conclusion

In this paper, we experimentally investigated link quality fluctuation in low-power wireless sensing networks deployed on the surface of different water bodies. We used waterproof boxes to seal some of the sensor nodes, so that they can operate in rough conditions (excessive rainfall and heat as well as rough water motion). We tested whether or not the boxes significantly affected link quality. Repeated experiments in different weather conditions revealed that the boxes, in fact, slightly improved link quality, both for the deployments we carried out on land and on the surface of water. We also observed that link quality was, by and large, more stable on the surface of water than on land, though the change in RSSI was proportional to the movement of water. Furthermore, even though the difference in performance was not appreciable, we observed that the choice of a power bank affected link quality. Our experiments with two different power banks, one small and one large, both in size and in capacity, persistently resulted in a slightly better performance when the big power bank was used, both for the land and for the water deployments. This was partly, due to imperfections – such as poor impedance matching – in the design of the smaller power bank. More generally, the change in link quality was proportional to the movement of water; the rougher the movement, the more significant the change. Using statistics collected in the absence of any mobility as measurement error and the changes in RSSI when the nodes were deployed on the water as process error,

we developed a Kalman Filter to predict the change in link quality. The results suggested that our approach was plausible. Our future work involves actual water quality monitoring. Work is already in progress to integrate water quality sensors into our sensor platforms.

References

[1] I. Bashir, F. A. Lone, R. A. Bhat, S. A. Mir, Z. A. Dar, and S. A. Dar, "Concerns and threats of contamination on aquatic ecosystems," *Bioremediation and Biotechnology*, vol. 27, pp. 1–26, 2020.

[2] S. W. H. Al-Muqdadi, "The spiral of escalating water conflict: The theory of hydro-politics," *Water*, vol. 14, no. 21, 2022, ISSN: 2073-4441. [Online]. Available: https://www.mdpi.com/2073-4441/14/21/3466.

[3] N. Akhtar, M. I. Syakir Ishak, S. A. Bhawani, and K. Umar, "Various natural and anthropogenic factors responsible for water quality degradation: A review," *Water*, vol. 13, no. 19, p. 2660, 2021.

[4] A. Fernandes, M. Figueiredo, J. Ribeiro, J. Neves, and H. Vicente, "Avoidance of operational sampling errors in drinking water analysis," *AQUA—Water Infrastructure, Ecosystems and Society*, vol. 71, no. 3, pp. 373–386, 2022.

[5] M. V. Storey, B. Van der Gaag, and B. P. Burns, "Advances in on-line drinking water quality monitoring and early warning systems," *Water research*, vol. 45, no. 2, pp. 741–747, 2011.

[6] A. T. Demetillo, M. V. Japitana, and E. B. Taboada, "A system for monitoring water quality in a large aquatic area using wireless sensor network technology," *Sustain Environ Res*, vol. 29, no. 12, 2019.

[7] H. Yang, J. Kong, H. Hu, Y. Du, M. Gao, and F. Chen, "A review of remote sensing for water quality retrieval: Progress and challenges," *Remote Sensing*, vol. 14, no. 8, p. 1770, 2022.

[8] V. Sagan, K. T. Peterson, M. Maimaitijiang, *et al.*, "Monitoring inland water quality using remote sensing: Potential and limitations of spectral indices, bio-optical simulations, machine learning, and cloud computing," *Earth-Science Reviews*, vol. 205, p. 103 187, 2020.

[9] Y. Chebud, G. M. Naja, R. G. Rivero, and A. M. Melesse, "Water quality monitoring using remote sensing and an artificial neural network," *Water, Air, & Soil Pollution*, vol. 223, pp. 4875–4887, 2012.

[10] J. Chen, M. Zhang, T. Cui, and Z. Wen, "A review of some important technical problems in respect of satellite remote sensing of chlorophyll-a concentration in coastal waters," *IEEE journal of selected topics in applied earth observations and remote sensing*, vol. 6, no. 5, pp. 2275–2289, 2013.

[11] S. Randhawa, S. S. Sandha, and B. Srivastava, "A multi-sensor process for in-situ monitoring of water pollution in rivers or lakes for high-resolution quantitative and qualitative water quality data," in *2016 IEEE Intl Conference on Computational Science and Engineering (CSE) and IEEE Intl Conference on Embedded and Ubiquitous Computing (EUC) and 15th Intl Symposium on Distributed Computing and Applications for Business Engineering (DCABES)*, 2016, pp. 122–129. DOI: 10.1109/CSE-EUC-DCABES.2016.171.

[12] E. Stump, J. S. Rosenfeld, and A. Vincent, "Habitat associations and threat vulnerabilities of seahorses and pipefishes (syngnathidae) in biscayne national park, florida, usa," *Bulletin of Marine Science*, 2023.

[13] C. Groppe, "Assessing the effects of thermal stress, hypoxia, and hydrogen sulfide exposure on the survival of the gulf toadfish (opsanus beta)," Ph.D. dissertation, University of Miami, 2022.

[14] G. Oikonomou, S. Duquennoy, A. Elsts, J. Eriksson, Y. Tanaka, and N. Tsiftes, "The contiki-ng open source operating system for next generation iot devices," *SoftwareX*, vol. 18, p. 101 089, 2022.

[15] R. Das, A. Gadre, S. Zhang, S. Kumar, and J. M. Moura, "A deep learning approach to iot authentication," in *2018 IEEE international conference on communications (ICC)*, IEEE, 2018, pp. 1–6.

[16] H. Bojinov, Y. Michalevsky, G. Nakibly, and D. Boneh, "Mobile device identification via sensor fingerprinting," *arXiv preprint arXiv:1408.1416*, 2014.

[17] M. Bucolo, A. Buscarino, C. Famoso, L. Fortuna, and M. Frasca, "Control of imperfect dynamical systems," *Nonlinear Dynamics*, vol. 98, pp. 2989–2999, 2019.

[18] Y. Yoon, H. Kim, H. Kim, K.-S. Lee, C.-H. Lee, and J. S. Kenney, "A 2.4-ghz cmos power amplifier with an integrated antenna impedance mismatch correction system," *IEEE Journal of Solid-State Circuits*, vol. 49, no. 3, pp. 608–621, 2014.

[19] W. Dargie and J. Wen, "Examination of indoor localization techniques and their model parameters," in *2021 IEEE 18th International Conference on Mobile Ad Hoc and Smart Systems (MASS)*, IEEE, 2021, pp. 364–373.

[20] L. Wang, Z. Chen, H. Zou, *et al.*, "A deep learning-based high-temperature overtime working alert system for smart cities with multi-sensor data," *Nondestructive Testing and Evaluation*, vol. 39, no. 1, pp. 164–184, 2024.

[21] W. Shen and B. Wen, "Experimental research of uhf radio back-scattered from fresh and seawater surface," *Progress in Electromagnetics Research M*, vol. 11, pp. 99–109, Jan. 2010. DOI: 10.2528/PIERM10010308.

[22] M. G. Gaitán, P. M. d'Orey, P. M. Santos, *et al.*, "Wireless radio link design to improve near-shore communication with surface nodes on tidal waters," in *OCEANS 2021: San Diego – Porto*, 2021, pp. 1–8. DOI: 10.23919/OCEANS44145.2021.9706046.

[23] K. Yang, A. F. Molisch, T. Ekman, T. Røste, and M. Berbineau, "A round earth loss model and small-scale channel properties for open-sea radio propagation," *IEEE Transactions on Vehicular Technology*, vol. 68, no. 9, pp. 8449–8460, 2019.

[24] X. Li, H. Song, and C. Liu, "Path loss modeling for wireless network deployment in water surface environments," *IEEE Antennas and Wireless Propagation Letters*, vol. 21, no. 6, pp. 1090–1094, 2022.

[25] B. Yamamoto, A. Wong, P. J. Agcanas, *et al.*, "Received signal strength indication (rssi) of 2.4 ghz and 5 ghz wireless local area network systems projected over land and sea for near-shore maritime robot operations," *Journal of Marine Science and Engineering*, vol. 7, no. 9, p. 290, 2019.

[26] S. Li, Y. Guo, and B. Bingham, "Multi-robot cooperative control for monitoring and tracking dynamic plumes," in *2014 IEEE International Conference on Robotics and Automation (ICRA)*, 2014, pp. 67–73. DOI: 10.1109/ICRA.2014.6906591.

[27] M. Jadaliha and J. Choi, "Environmental monitoring using autonomous aquatic robots: Sampling algorithms and experiments," *IEEE Transactions on Control Systems Technology*, vol. 21, no. 3, pp. 899–905, 2013. DOI: 10.1109/TCST.2012.2190070.

[28] G. Xu, W. Shen, and X. Wang, "Applications of wireless sensor networks in marine environment monitoring: A survey," *Sensors*, vol. 14, no. 9, pp. 16 932–16 954, 2014, ISSN: 1424-8220. DOI: 10.3390/s140916932. [Online]. Available: https://www.mdpi.com/1424-8220/14/9/16932.

[29] A. Shahanaghi, Y. Yang, and R. M. Buehrer, "Stochastic link modeling of static wireless sensor networks over the ocean surface," *IEEE Transactions on Wireless Communications*, vol. 19, no. 6, pp. 4154–4169, 2020. DOI: 10.1109/TWC.2020.2979974.

[30] U. M. Cella, N. Shuley, and R. Johnstone, "Wireless sensor networks in coastal marine environments: A study case outcome," in *Proceedings of the 4th International Workshop on Underwater Networks*, ser. WUWNet '09, Berkeley, California: Association for Computing Machinery, 2009, ISBN: 9781605588216. DOI: 10.1145/1654130.1654138. [Online]. Available: https://doi.org/10.1145/1654130.1654138.